

УЧЕБНИК

ЛУЧЕВАЯ ДИАГНОСТИКА

Под редакцией профессора Г.Е. Труфанова

3-е издание, переработанное и дополненное

Министерство науки и высшего образования РФ

Рекомендовано ФГАУ «Федеральный институт развития образования»
в качестве учебника для использования в образовательном процессе
образовательных организаций, реализующих программы высшего образования
по специальностям 31.05.01 «Лечебное дело»,
31.05.02 «Педиатрия», 31.05.03 «Стоматология»,
32.05.01 «Медико-профилактическое дело»

TEXTBOOK

DIAGNOSTIC RADIOLOGY

Editor
Professor G.E. Trufanov



Moscow
«GEOTAR-Media»
PUBLISHING GROUP
2021

CONTENTS

Authors	13
Introduction	15
List of abbreviations and symbols	16
Chapter 1. General principles and contents of diagnostic radiology.	
Organization of imaging studies	17
1.1. General principles of diagnostic radiology	19
1.2. The fundamental procedure for the study of radiation image.....	21
1.3. Organization of imaging studies	25
Practice questions	26
Chapter 2. Fundamentals and clinical application of radiological diagnostic method	27
2.1. Methods of radiological examination	30
2.1.1. General methods of radiological examination.....	31
2.1.2. Special methods of radiological examination	36
2.1.3. Methods involving the use of artificial contrast	37
2.2. Indications for radiological method	43
Practice questions	46
Chapter 3. Principles and clinical use of ultrasound examination	47
3.1. The history of ultrasound examination	48
3.2. Principles of ultrasound examination	49
3.3. Modes of ultrasound imaging	50
3.4. Principles of image interpretation during ultrasound examination	53
3.5. Indications for ultrasound examination	56
Practice questions	59
Chapter 4. Principles and clinical application of X-ray computed tomography	60
4.1. Preparation of a patient	65
4.2. General methodology of computed tomography examination.....	66
4.3. Methods of contrast enhancement of images	67
4.4. Special techniques of computed tomography.....	68
4.5. Indications for computed tomography	71
Practice questions	75
Chapter 5. Principles and clinical use of magnetic resonance imaging	76
5.1. Physical basis of magnetic resonance imaging	77
5.2. Contrast agents.....	81
5.3. Techniques of magnetic resonance imaging	82
5.3.1. Basic techniques	82
5.3.2. Special techniques	83
5.4. Contraindications to magnetic resonance imaging	84
5.5. Advantages of magnetic resonance imaging	85
5.6. Disadvantages of magnetic resonance imaging	85
5.7. Indications for magnetic resonance imaging	85
Practice questions	88

Chapter 6. Foundations and clinical applications of radionuclide method of diagnosis ...	89
6.1. Physical basis of the radionuclide method of diagnosis.....	89
6.2. Radionuclide examinations based on the γ -emitting nuclides	90
6.2.1. The main types of machines and the principles of γ -quanta registration ...	91
6.2.2. The γ -quantum registration.....	92
6.2.3. Types of radionuclide examinations	93
6.2.4. Applications of single-photon emission computed tomography.....	93
6.2.5. Indications for radionuclide examinations.....	99
6.3. Radionuclide examinations based on positron-emitting nuclides	101
6.3.1. Physical basis, principles of radiation detection and imaging in positron emission tomography.....	101
6.3.2. Methods of research in positron emission tomography.....	102
6.3.3. Radiopharmaceuticals for positron emission tomography	103
6.3.4. Basics of clinical application of positron emission tomography	104
6.3.5. Indications for positron emission tomography	106
Practice questions	106
Chapter 7. Diagnostic radiology of diseases and injuries of the musculoskeletal system	107
7.1. Methods of imaging study.....	107
7.1.1. The radiological method	107
7.1.2. X-ray computed tomography	108
7.1.3. Ultrasonic method	108
7.1.4. Magnetic resonance imaging.....	108
7.1.5. Radionuclide method	108
7.2. Normal radial musculoskeletal anatomy.....	109
7.3. Age-specific changes in the musculoskeletal system.....	113
7.4. General radiological semiotics of pathological changes in the musculoskeletal system	115
7.4.1. General radiological semiotics	115
7.4.2. General ultrasound semiotics	119
7.4.3. General magnetic resonance semiotics.....	120
7.4.4. General semiotics of pathological changes in radionuclide examination.....	122
7.5. Radiological semiotics of diseases of the musculoskeletal system	123
7.5.1. Acute hematogenous osteomyelitis.....	123
7.5.2. Whitlow	126
7.5.3. Osteoarticular tuberculosis.....	127
7.5.4. Acute infectious suppurative arthritis	129
7.5.5. Rheumatoid Arthritis	129
7.5.6. Tumor diseases	130
7.5.7. Congenital dysplasia	136
7.5.8. Degenerative-dystrophic diseases.....	137
7.5.9. Endocrine and metabolic diseases	140
7.5.10. Exogenous intoxication	140
7.6. Radiological semiotics of soft tissues diseases	140
7.6.1. Abscesses and phlegmons.....	140
7.6.2. Bursitis, tenosynovitis, tendinitis, tendinosis	141
7.6.3. Soft tissue tumors.....	142

7.7. Radiological semiotics of damages to the musculoskeletal system	144
7.7.1. Bone fractures.....	144
7.7.2. Dislocations.....	150
7.7.3. Soft-tissue damages.....	152
Practice questions	156
Chapter 8. Diagnostic radiology of pulmonary and mediastinal diseases and injuries	157
8.1. Methods of imaging study	157
8.1.1. Radiological method.....	157
8.1.2. X-ray computed tomography	170
8.1.3. Magnetic resonance imaging	172
8.1.4. Ultrasound technique	172
8.1.5. Radionuclide method	173
8.2. Radiological semiotics of diseases of the lungs, pleura and mediastinum	175
8.2.1. Acute pneumonia	175
8.2.2. Acute pulmonary abscess	175
8.2.3. Bronchiectasis	176
8.2.4. Pulmonary emphysema	176
8.2.5. Focal pneumosclerosis.....	177
8.2.6. Diffusive interstitial disseminated diseases of the lungs	177
8.2.7. Pneumoconioses.....	178
8.2.8. Thromboembolism of the pulmonary artery.....	178
8.2.9. Pulmonary edema.....	180
8.2.10. Central lung cancer.....	180
8.2.11. Peripheral lung cancer	181
8.2.12. Hematogenous metastases of malignant tumors in lungs.....	182
8.2.13. Pulmonary tuberculosis	182
8.2.14. Exudative pleuritis	186
8.2.15. Spontaneous pneumothorax	187
8.2.16. Mediastinal neoplasms	187
8.3. Radiological semiotics of the lung and pleura injuries	189
8.3.1. Pneumothorax.....	189
8.3.2. Hemothorax	189
8.3.3. Hemopneumothorax.....	190
8.3.4. Pulmonary contusion.....	190
8.3.5. Lung laceration.....	191
Practice questions	191
Chapter 9. Diagnostic radiology of the heart and thoracic aorta diseases and injuries ...	192
9.1. Methods of imaging study	192
9.1.1. Radiological method.....	192
9.1.2. Ultrasound technique	203
9.1.3. X-ray computed tomography.....	206
9.1.4. Magnetic resonance imaging.....	209
9.1.5. Radionuclide method	210
9.2. Radiological semiotics of the heart and thoracic aorta diseases	212
9.2.1. Coronary heart disease	212
9.2.2. Acute myocardial infarction.....	213
9.2.3. Mitral stenosis	213
9.2.4. Mitral valve insufficiency	214

9.2.5. Aortic valve stenosis	215
9.2.6. Aortic valve insufficiency	215
9.2.7. Pericardial effusion	216
9.2.8. Adhesive constrictive pericarditis	216
9.2.9. Thoracic aorta aneurisms	217
9.3. Radiological semiotics of the heart and thoracic aorta injures	217
9.3.1. Contusion of the heart	217
9.3.2. Rupture of the external walls of the heart	218
9.3.3. Rupture of the thoracic aorta	218
Practice questions	218
Chapter 10. Diagnostic radiology of diseases and injuries of the pharynx, esophagus, stomach and intestines	219
10.1. Methods of imaging study	219
10.1.1. Radiological method	219
10.1.2. Computed tomography	228
10.1.3. Magnetic resonance imaging	228
10.1.4. Ultrasound technique	229
10.1.5. Radionuclide technique	229
10.2. Radiological semiotics of diseases of the esophagus, stomach and intestines	230
10.2.1. Diseases of the esophagus	230
10.2.2. Diseases of the stomach	238
10.2.3. Enteropathy	245
10.3. Radiological semiotics of damage to the pharynx, esophagus, stomach and intestines	253
10.3.1. Hollow organ perforation	255
10.3.2. Acute intestinal obstruction	255
Practice questions	257
Chapter 11. Diagnostic radiology of diseases and injuries of digestive parenchymatous organs	258
11.1. Liver	258
11.1.1. Radiological anatomy in normal condition	258
11.1.2. Methods of imaging study	260
11.1.3. Radiological semiotics of liver and biliary tract diseases	266
11.1.4. Radiological semiotics of liver and biliary tract damage	273
11.2. Pancreas gland and spleen	275
11.2.1. Radiological methods	275
11.2.2. Radiological semiotics of pancreatic diseases	279
11.2.3. Radiological semiotics of the spleen diseases	282
11.2.4. Radiological semiotics of the pancreas damages	283
11.2.5. Radiological semiotics of the spleen damages	284
Practice questions	284
Chapter 12. Diagnostic radiology of diseases and injuries of urinary organs	285
12.1. Methods of radiation diagnosis in urology	285
12.1.1. Radiological method	285
12.1.2. Ultrasound technique	292
12.1.3. X-ray computed tomography	293

12.1.4. Magnetic resonance imaging	295
12.1.5. Radionuclide technique	296
12.2. Radiological semiotics of diseases of urinary organs	300
12.2.1. Kidney duplication	300
12.2.2. Ectopic kidney	301
12.2.3. Nephroptosis	301
12.2.4. Nephroptosis	303
12.2.5. Chronic pyelonephritis	303
12.2.6. Tuberculosis of the kidney	304
12.2.7. Urolithiasis	304
12.2.8. Hydronephrosis	304
12.2.9. Kidney tumor	306
12.2.10. Renal cyst	307
12.2.11. Polycystic disease in adults (polycystic kidney disease)	308
12.2.12. Bladder tumor	309
12.3. Radiological semiotics of damage to the urinary organs	309
12.3.1. Kidney damage	309
12.3.2. Subcapsular hematoma	310
12.3.3. Rupture of the parenchyma	311
12.3.4. Rupture of the kidney with damage to the pyelocaliceal complex	311
12.3.5. Crushing of injury to the kidneys, avulsion to the renal pedicle or thrombosis of the renal artery	311
12.3.6. Damage to the ureters	311
12.3.7. Damage to the bladder	312
12.3.8. Damage to the urethra	313
Practice questions	313
Chapter 13. Diagnostic radiology of diseases and injuries of sex organs	314
13.1. Diagnostic radiology in andrology	314
13.1.1. Radiological method	314
13.1.2. Ultrasonic method	315
13.1.3. X-ray computed tomography	315
13.1.4. Magnetic resonance imaging	315
13.1.5. Radionuclide method	316
13.2. Radiological semiotics of diseases of male sex organs	316
13.2.1. Cryptorchidism	316
13.2.2. Urethral stricture	316
13.2.3. Recurrent varicocele	316
13.2.4. Testicular torsion	317
13.2.5. Acute prostatitis	318
13.2.6. Chronic prostatitis	318
13.2.7. Benign prostatic hyperplasia	318
13.2.8. Prostate cancer	318
13.2.9. Testicular tumor	319
13.2.10. Erectile dysfunction	320
13.3. Radiological semiotics of injuries of male sex organs	320
13.4. Diagnostic radiology in gynaecology	320
13.4.1. Radiological method	320
13.4.2. Ultrasonic method	321
13.4.3. X-ray computed tomography	322

13.4.4. Magnetic resonance imaging	322
13.4.5. Radionuclide method	322
13.5. Radiological semiotics of diseases of the female sex organs	323
13.5.1. Didelphia	323
13.5.2. Salpingitis	323
13.5.3. Uterine myoma	324
13.5.4. Endometrial cancer	324
13.5.5. Ovarian cancer	325
13.5.6. Endometriosis	325
13.5.7. Inflammatory diseases of the breast: mastitis, abscess	326
13.5.8. Breast cancer	326
13.6. Radiological semiotics of damages to the female sex organs	327
13.7. Diagnostic radiology in obstetrics	327
13.7.1. Ultrasonic method	328
13.7.2. Magnetic resonance imaging	328
13.8. Radiological semiotics of pregnancy pathology	328
13.8.1. Extrauterine pregnancy	328
13.8.2. Missed miscarriage	328
13.8.3. Molar pregnancy	328
13.8.4. Placental abruption	328
Practice questions	329
Chapter 14. Diagnostic radiology of craniocerebral diseases and injuries	330
14.1. Methods of diagnostic radiology	330
14.1.1. Radiological method	330
14.1.2. X-ray computed tomography	335
14.1.3. Special CT techniques	336
14.1.4. Magnetic resonance imaging	337
14.1.5. Radionuclide method	339
14.1.6. Ultrasound method	341
14.2. Radiological semiotics of the brain diseases	341
14.2.1. Brain tumors	341
14.2.2. Demyelinating diseases	345
14.2.3. Cerebrovascular diseases	346
14.2.4. Infectious diseases	350
14.2.5. Parasitic diseases (cysticercosis, toxoplasmosis)	352
14.3. Radiological semiotics of craniocerebral diseases and injuries	352
14.3.1. Calvarial bones and skull base fractures	352
14.3.2. Brain damages	356
Practice questions	359
Chapter 15. Diagnostic radiology of diseases and injuries of the spine and spinal cord	360
15.1. Methods of diagnostic radiology	360
15.1.1. Radiological method	360
15.1.2. X-ray computed tomography	363
15.1.3. Magnetic resonance imaging	364
15.1.4. Radionuclide method	366
15.2. Radiological semiotics of diseases of the spinal cord	366
15.2.1. Spinal tumors	366
15.2.2. Demyelinating diseases	368

15.2.3. Inflammatory diseases	368
15.2.4. Vascular diseases	372
15.2.5. Intramedullary cysts	374
15.2.6. Degenerative-dystrophic disease of the spine.....	375
15.3. Radiological semiotics of spine and spinal cord injuries	378
15.3.1. Injury of cervical spine	378
15.3.2. Damage to the thoracic and lumbar spine.....	379
15.3.3. Spinal cord injury	381
Practice questions	381
Chapter 16. Diagnostic radiology of diseases and injuries of the visual organ	382
16.1. Methods of diagnostic radiology	382
16.1.1. Radiological method	382
16.1.2. X-ray computed tomography	384
16.1.3. Magnetic resonance imaging	385
16.1.4. Ultrasonic method	386
16.1.5. Radionuclide method	386
16.2. Radiological semiotics of eye and orbit injuries	386
16.2.1. Fractures of the walls of the orbit	386
16.2.2. Foreign bodies.....	387
16.2.3. Intraocular hemorrhages.....	388
16.2.4. Traumatic retinal detachment.....	389
16.3. Radiological semiotics of eye and orbit diseases	390
16.3.1. Tumor of the choroid of the eye (melanoblastoma)	390
16.3.2. Tumors of the orbit	391
16.3.3. Dacryocystitis	392
16.3.4. Endocrine ophthalmopathy	392
Practice questions	392
Chapter 17. Diagnostic radiology of diseases and injuries of ENT organs	393
17.1. Methods of diagnostic radiology	393
17.1.1. Radiological method	393
17.1.2. X-ray computed tomography	394
17.1.3. Magnetic resonance imaging	395
17.2. Radiological semiotics of diseases of ENT organs.....	396
17.2.1. Radiological semiotics of diseases of the ear	396
17.2.2. Radiological semiotics of diseases of the nose and paranasal sinuses ...	398
17.2.3. Radiological semiotics of pharyngeal and laryngeal diseases	401
17.3. Radiological semiotics of injuries of ENT organs.....	402
17.3.1. Injuries and foreign bodies of temporal bones.....	402
17.3.2. Damage and foreign bodies of the paranasal sinuses	403
17.3.3. Damage to the larynx.....	403
Practice questions	403
Chapter 18. Radiological diagnosis of diseases and injuries of the maxillofacial region.....	404
18.1. Methods of diagnostic radiology	404
18.1.1. Radiological methods	404
18.1.2. X-ray computed tomography	406
18.1.3. Magnetic resonance imaging.....	407
18.1.4. Ultrasonic method	408

18.2. Radiological semiotics of diseases of maxillofacial region	408
18.2.1. Caries	408
18.2.2. Fluorosis, enamel and dentin hypoplasia, crown erosion, cuneated defects of dental necks	408
18.2.3. Pulpitis, periodontitis	408
18.2.4. Granulating osteitis, granulomatous osteitis, fibrous osteitis, periostitis of the jaw	408
18.2.5. Osteomyelitis of the jaws	409
18.2.6. Inflammatory-dystrophic and idiopathic changes in periodontium- gingivitis	409
18.2.7. Periodontitis and periodontal disease, periodontitis.....	409
18.2.8. Cysts and soft tissue tumors of the jaws	410
18.2.9. Metastases and cancer of the jaw	410
18.2.10. Impacted teeth, fragments of dental roots	410
18.2.11. Calcifications, salivary stones on the teeth	411
18.2.12. Dense odontogenic tumors, dense osteogenic tumors	411
18.2.13. Deforming arthrosis, arthritis of the temporomandibular joint.....	411
18.2.14. Ankylosis, contracture of the temporomandibular joint	412
18.2.15. Malformations of the salivary glands, sialoadenitis, salivary stone disease, fistulas of the salivary glands.....	412
18.2.16. Cysts and tumors of the salivary glands	412
18.3. Radiological semiotics of damage to the bones of the facial skeleton and teeth	413
18.3.1. Fractures of the bones of the upper zone of the facial skeleton	413
18.3.2. Fractures of the bones of the middle zone of the facial skeleton	415
18.3.3. Fractures of the lower jaw	416
18.3.4. Fractures and dislocations of teeth	417
18.3.5. Dislocation of the lower jaw	418
Practice questions	419
Chapter 19. Radiation safety during radiological and radionuclide diagnostic studies ...	419
19.1. Initial prerequisites	419
19.1.1. Physical concepts and dosimetric quantities	419
19.1.2. Medical effects of human irradiation.....	423
19.1.3. Doses that consider the biological effect	425
19.1.4. The operational dosimetric quantities	427
19.2. Principles and norms of radiation safety	428
19.2.1. General principles of radiation safety	428
19.2.2. Radiation safety norms	429
19.2.3. Safe and reference limits and intervention limits	431
19.3. Radiation safety in radiology and nuclear medicine departments	432
19.4. Evaluation of patient and staff radiation doses	434
Practice questions	437
References.....	438

Chapter 9

DIAGNOSTIC RADIOLOGY OF THE HEART AND THORACIC AORTA DISEASES AND INJURIES

9.1. METHODS OF IMAGING STUDY

Different techniques can be implemented in the imaging study of the heart and thoracic aorta. Each technique has its advantages and disadvantages. The technique is chosen according to certain clinical settings, to resolve particular diagnostic tasks.

9.1.1. Radiological method

The radiologic technique, despite new highly informative ways of receiving medical images, is still widely spread in the examination of the heart and thoracic aorta. However, many of the previously used radiologic techniques are not used any more. Only the simplest, native techniques (radiography, fluoroscopy) and the most complicated, invasive contrast examinations — angiocardiography, coronography and aortography have preserved the diagnostic value.

Native radiological methods

Radiography is, as a rule, the primary technique of imaging study of the heart and thoracic aorta. The currently accepted views are frontal and left lateral. Fluoroscopy is used when it is necessary to choose a non-standard optimal view for the study of a particular part of the cardiovascular shadow and for an indicative assessment of the contractile function of the heart and aortic pulsation. In addition, radioscopy has more opportunities to identify calcifications of the heart valves. Native X-ray examination of the thoracic aorta in the absence of CT can be supplemented by linear tomography. Indications for its implementation are the need to clarify the details of the morphological state of the aorta (expansion, narrowing, calcification of the walls, etc.) and the difficulties of differential diagnosis with the pathological processes of other organs of the thoracic cavity, most often with neoplasms of the mediastinum.

Normal radioanatomy of the heart and thoracic aorta

As cardiac chambers and aorta have the same density, in native radiological examination they produce a cumulative homogeneous shadow. It helps to determine the location, shape and size of the heart and aorta in general.

The location of the heart silhouette in frontal view is mid-asymmetric: 1/3 of it is located to the right of the median line, 2/3 is to the left. The left heart border does not reach the mamillary line by 1.5–2 cm, and the right border is separated from the

middle vertical line to the right by no more than 5 cm. Above the shadow of the heart, as if coming out of it, there is a cardiovascular shadow formed by the thoracic aorta, the upper vena cava and the pulmonary artery. The upper contour of this shadow does not reach the left sternoclavicular joint on 1.5–2 cm — the ratio of the heights cardiac and vascular segments are 1:1.

The location, shape and size of the heart are influenced by the constitutional type, respiratory phase and body positioning.

In order to evaluate the location of the heart depending on its constitutional type, the so-called inclination angle is determined. It is formed by the longitudinal axis of the heart and horizontal line, which is passing through the height of the heart silhouette. The heart in the normosthenic body is located obliquely, in hypersthenic it is more horizontally located, in asthenic; on the contrary, it has a more upright position. The angles of inclination of the heart are respectively 45° , less than 40° , more than 50° (Fig. 9.1).

Respiratory phase and body positioning change the heart location due to the different diaphragm height. In the vertical position of the patient and on inspiration, the diaphragm descends, and the heart takes a vertical position. In the horizontal position

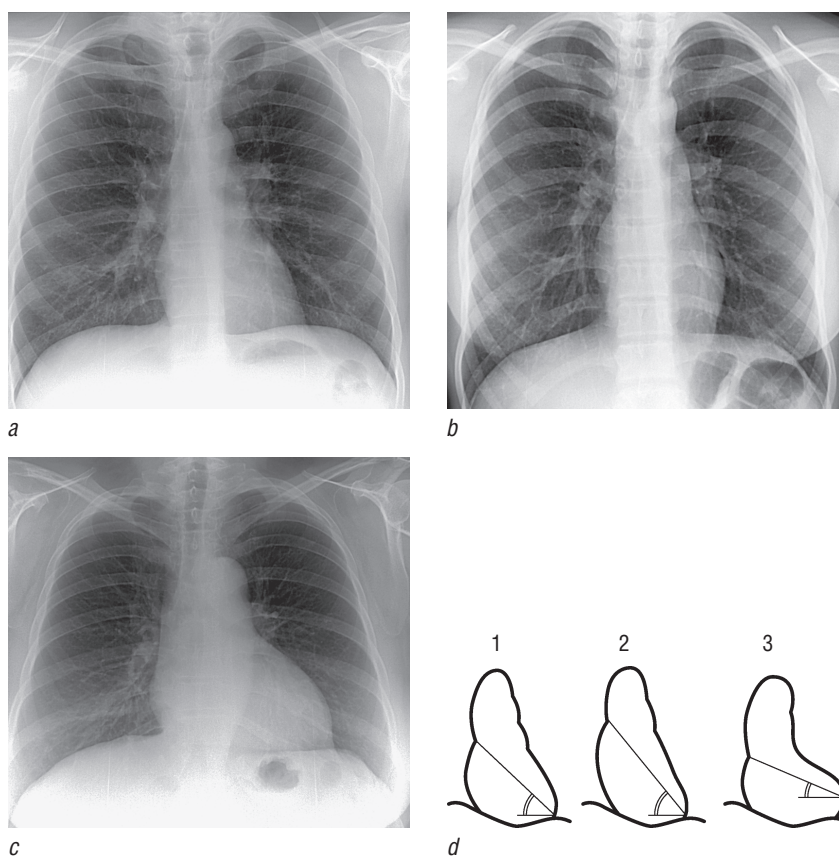


Fig. 9.1. Frontal chest X-ray with different heart positioning due to the constitutional type: *a* — normosthenic; *b* — asthenic; *c* — hypersthenic; *d* — schemes (1 — normosthenic, 2 — asthenic, 3 — hypersthenic)

of the patient and on exhalation, the diaphragm rises, and the heart takes a more horizontal position (Fig. 9.2).

The changes in heart location can be caused by the different pathological processes in annexa and anatomical structures, such as chest distortion (kyphosis, scoliosis, hollowed chest), respiratory, pleura, diaphragm diseases, which are accompanied by the volumetric changes (atelectasis or cirrhosis of the lungs, exudative pleurisy, pneumothorax, diaphragmatic hernia) (Fig. 9.3, 9.4).

In frontal view, the right border consists of two arches; the ascending aorta forms the upper arch, and the lower is formed by right atrium. The point of intersection of these arches is called the right cardiovascular angle. The left contour is formed by four arches: the upper skiological arch is formed not as much by the anatomical arch of the aorta as by its descending part; below its second arch is formed by the main trunk and the left branch of the pulmonary artery; even lower is the short arch of the left atrium eyelet; the lowest and longest arch is formed by the left ventricle. The second and third

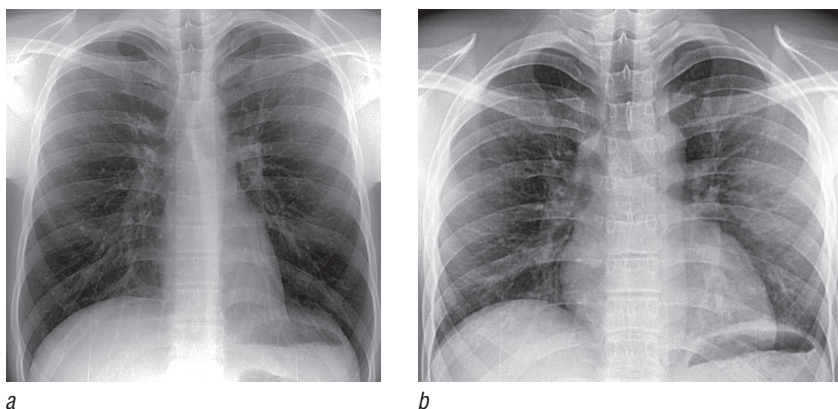


Fig. 9.2. Frontal chest X-ray: *a* — at full inspiratory effort; *b* — at a full expiratory effort

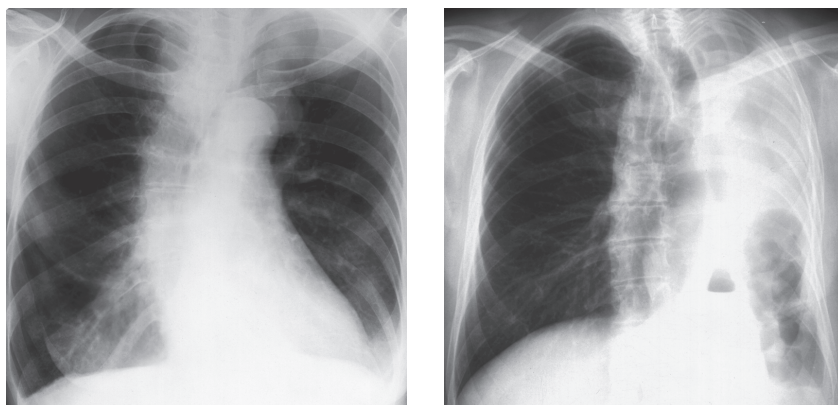


Fig. 9.3. Frontal X-ray. Left-sided scoliosis of the thoracic spine

Fig. 9.4. Frontal X-ray. Left-sided fibrothorax

arches form the “waist” of the heart. The point of their intersection is called the left cardiovascular angle (Fig. 9.5).

In the left lateral view cardiovascular silhouette has a shape of obliquely positioned oval adjacent to the diaphragm and sternum. Its frontal border is: at the top — the ascending part of the aorta, below — the right ventricle. The posterior border is formed at the top by the left atrium, below — by the left ventricle (Fig. 9.6).

The shape of cardiovascular silhouette undergoes significant changes due to the different diseases. The important thing is that these changes are typical of certain dis-

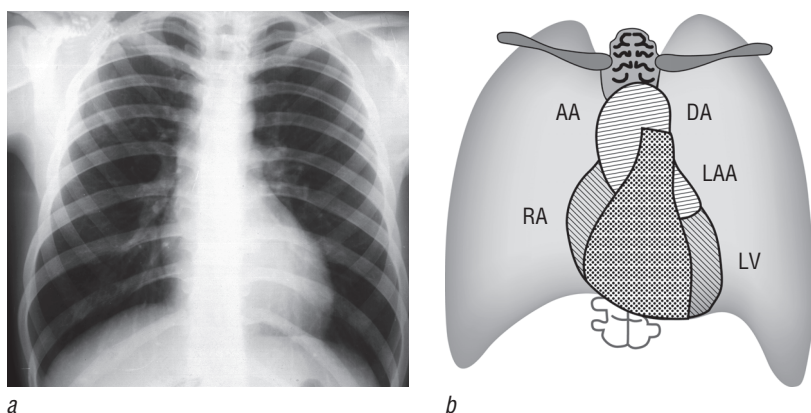


Fig. 9.5. X-ray (a) and scheme (b) of the chest in frontal view with the designation of the heart arches. AA — ascending aorta; RA — right atrium; DA — descending aorta; LAA — left atrial appendage; LV — left ventricle

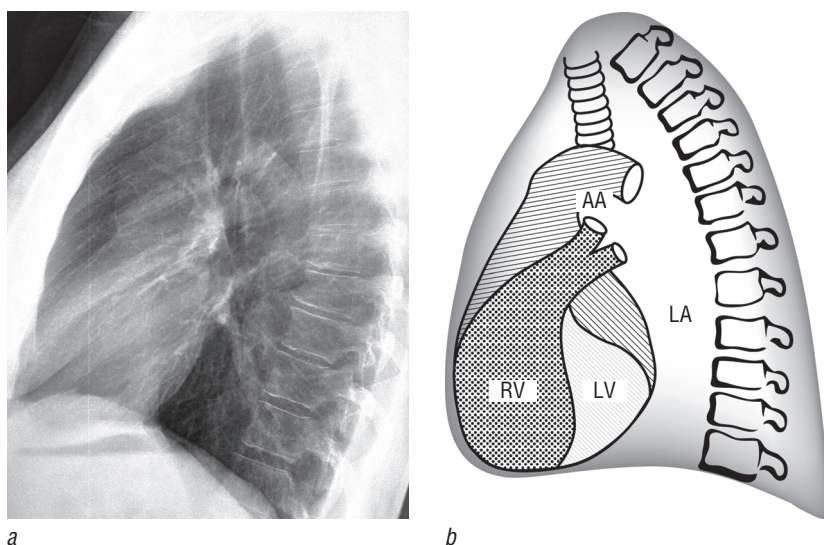


Fig. 9.6. X-ray (a) and scheme (b) of the chest in left lateral view with the designation of the heart arches. AA — ascending aorta; RV — right ventricle; LA — left atrium; LV — left ventricle

eases, which can be suspected at the first approximate assessment of the heart shape. There are five types of pathological shape of the cardiovascular silhouette in frontal view, such as the mitral, aortic, circular-shaped, trapezius (triangulate) and shape with local expansion, which is untypical of any cardiac chambers.

Basic features of mitral configuration of the heart:

- ▶ elongation and nipple of the second and third arches of the left contour of the heart silhouette;
- ▶ the upward displacement of the right cardiovascular angle as a result of the exit to the right contour of the enlarged left atrium, an increase in the right atrium or its displacement by the enlarged right ventricle (Fig. 9.7).

Such an image is displayed by mitral diseases (classic case is mitral stenosis), some congenital malformations that are accompanied by the left-to-right shunt (patent arterial duct, septal defect) and the so-called pulmonary heart, which is a consequence of pulmonary hypertension in diffuse chronic lung diseases.

Signs of aortic configuration:

- ▶ retraction of the waist of the heart;
- ▶ extension of the lower arch along the left border;
- ▶ increase and nipple of the upper arch on the right and shift down of the right cardiovascular angle that is caused by the expansion of the ascending aorta (Fig. 9.8).

This type of cardiovascular silhouette is a characteristic of aortic malformations, hypertrophic cardiomyopathy, aortic coarctation, hypertension and atherosclerotic cardiosclerosis.

Spherical shape, in combination with an increase in heart size is characteristic of pericardial effusion, multi-valvular acquired heart diseases (Fig. 9.9).

Trapezius (triangulate) shape is common in diffuse myocardium damage (myocarditis, myocardiodystrophy, myocardiosclerosis) (Fig. 9.10, 9.11).

Aneurysms of the heart and aorta, tumors and cysts of the heart, neoplasms of the mediastinum, adjacent to the heart and aorta are manifested by the local expansion of the cardiovascular silhouette (Fig. 9.12, 9.13).

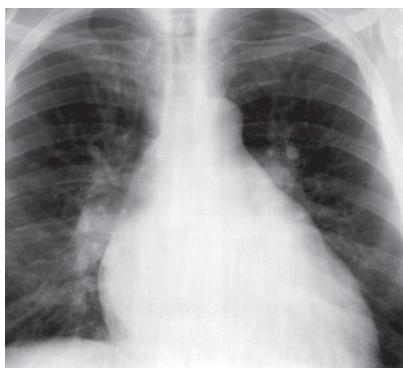


Fig. 9.7. Frontal X-ray. Mitral heart configuration

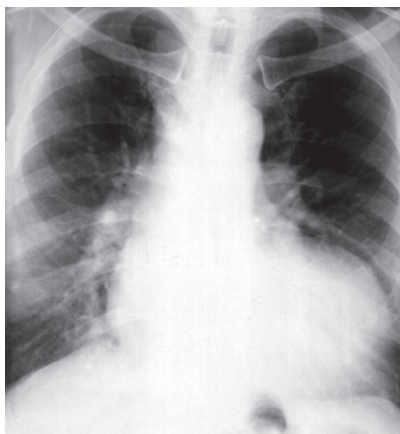


Fig. 9.8. Frontal X-ray. Aortic heart configuration

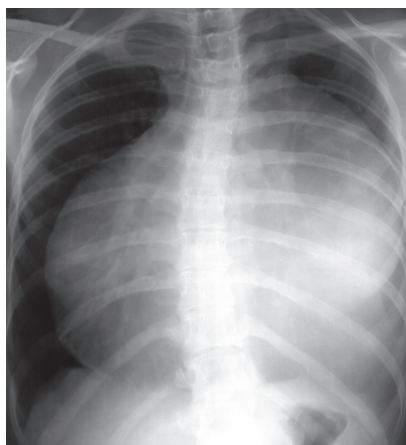


Fig. 9.9. Frontal X-ray. Spherical configuration of the heart

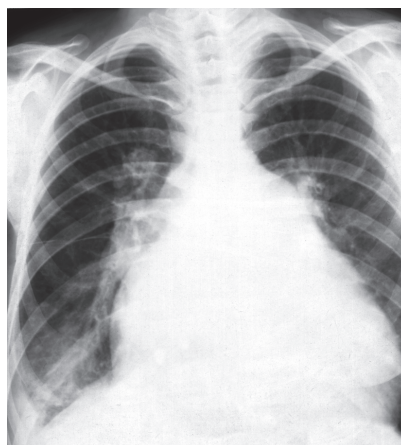


Fig. 9.10. Frontal X-ray. Trapeziform configuration of the heart

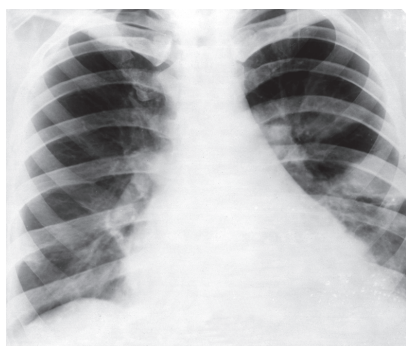


Fig. 9.11. Frontal X-ray. The triangular configuration of the heart

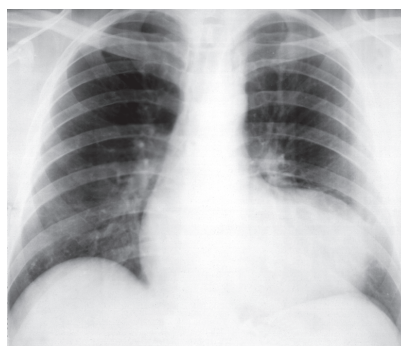


Fig. 9.12. Frontal X-ray. Local expansion of the heart silhouette due to aneurysm of the left ventricle of the heart

Various pathological processes of the aorta are manifested by five main radiological signs: elongation, arcuation, rotation, expansion, increase of the intensity of the shadow.

The elongation of the aorta is evidenced by a decrease in the distance from the upper contour of the aortic arch to the left sternoclavicular joint (less than 1 cm). The bending of the aorta is the result of its significant elongation, whereby it bends to the right, going into the right pulmonary field.

This pattern simulates the expansion of the ascending aorta, although in fact, its diameter may be normal. When the aorta rotates, the aortic loop, normally going from front to back at an angle of 50–60°, straightens and approaches the frontal plane. As a result, the border of the descending aorta moves to the left. Expansion of the aorta in a frontal view may be accompanied by its protrusion into the right and left pulmonary fields. However, firstly, this may not happen in case of its actual expansion, and

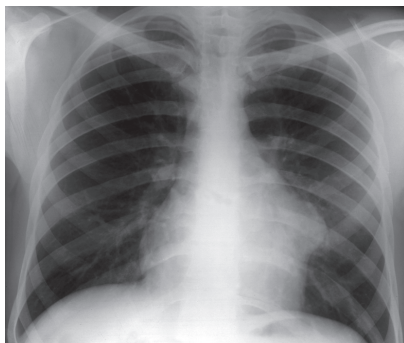


Fig. 9.13. Frontal X-ray. Local expansion of the heart silhouette due to exocardiac tumor

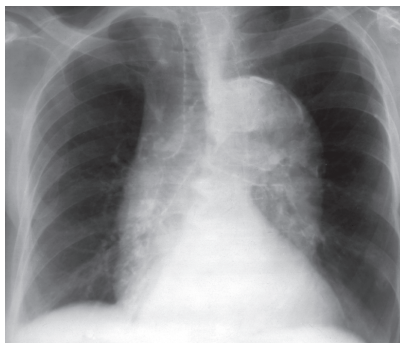


Fig. 9.14. Frontal X-ray. Lengthening, arcuation, rotation, expansion of the thoracic aorta



Fig. 9.15. X-ray in lateral view. Induration of the walls of the thoracic aorta along its entire length

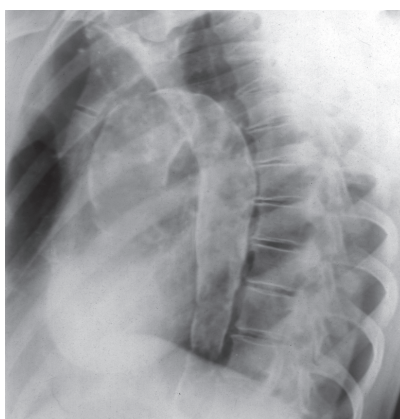


Fig. 9.16. X-ray in oblique lateral view. Calcification of the walls of the thoracic aorta along its entire length

secondly, this pattern is conditioned to a greater extent by the bending and unfolding of the aorta (Fig. 9.14). The increase in the intensity of the shadow is mainly connected with an increase in blood mass in the enlarged aorta and the induration of the vessel wall. At the same time, the descending aorta, in normal condition visible only in the initial part begins to be visualized in the lateral and oblique views over an increasing length. The most intense shadow is given by the calcifications of the wall (Fig. 9.15, 9.16).

The size is one of the most important indications of the condition of the whole heart as well as its chambers.

The general size of the heart can be evaluated with the help of frontal X-ray by cardiothoracic ratio $C/D \times 100\%$, where C is the diameter of the heart, measured horizontally between the most distant points of the right and left contours of the heart silhouette; D is the basal transverse size of the thoracic cage measured between the internal surfaces of the sidewalls of the chest cavity at the level of the right cardiophrenic angle (Fig. 9.17) For adults in normal condition this coefficient does not

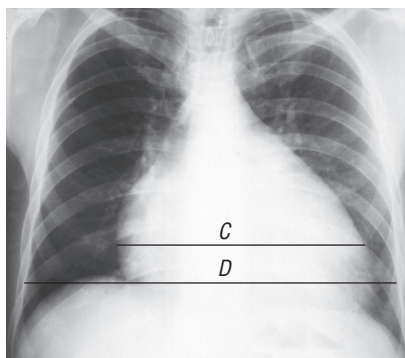


Fig. 9.17. Frontal X-ray with the designation of the measurements determining cardiothoracic ratio, where C is a heart breadth and D is the diametrical basal size of the thoracic cage

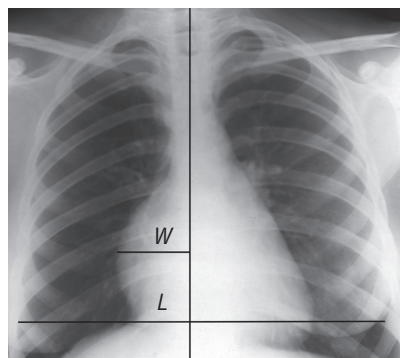


Fig. 9.18. Frontal X-ray with the designation of the measurements determining augmentation ratio of the right atrium: L — half of the diametrical basal size of the thoracic cage; W — the distance from the median line to the most distant point of the arch of the right atrium

exceed 50%. The increase in the first degree is up to 55% and the second is 60%, the thirds is more than 60%.

Right atrium. On frontal X-ray, the increase of the right atrium is manifested by the elongation and more significant protrusion of the bottom arch of the right border of the heart silhouette into the lung field, and by moving up of the right cardiovascular angle. More precisely, the degree of increase in the right atrium can be estimated using the Goodwin coefficient as the ratio (in percentage) of the distance from the median line to the most distant point of the arch of the right atrium W , to the half of the diametrical basal size of the thoracic cage L (Fig. 9.18): $W/L \times 100\%$. In normal condition, this ratio does not exceed 30%, with the expansion of the right atrium of the I degree it reaches 40%, II degree — 50%, III degree — more than 50%.

Right ventricle. In the frontal view, the right ventricle has no representation on the borders of the heart silhouette. Nevertheless, its increase is still displayed. First, the arch of the left ventricle shifts to the left, which is conditioned by either its displacement by the enlarged right ventricle or its direct exit to the border of the heart. Secondly, the right atrium is pushed to the right and upwards, which is accompanied by elongation and nipple of its arch and displacement of the right cardiovascular angle upwards. In the left lateral view, the size of the right ventricle is determined by the degree of its adhesion to the anterior thoracic wall. In normal condition, this contact does not exceed 1/4 of the length of the sternum. It is increasing with an enlargement of the right ventricle (Fig. 9.19).

Left atrium. In frontal view, enlargement of the left atrial leads to the lengthening of its arch on the left border. Also, there is an additional arch on the right border of the heart in the area of the right cardiovascular angle. At first, it is located more medial to the border of the heart, then crosses it, and at very large sizes becomes its cornerstone (Fig. 9.20). In the left lateral view, the size of the left atrium can be determined by the position of the esophagus. In normal condition, it has a rectilinear course, which is

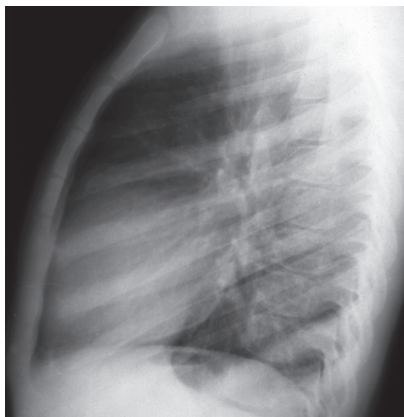


Fig. 9.19. X-ray in the left lateral view. The expansion of the right ventricle of the heart

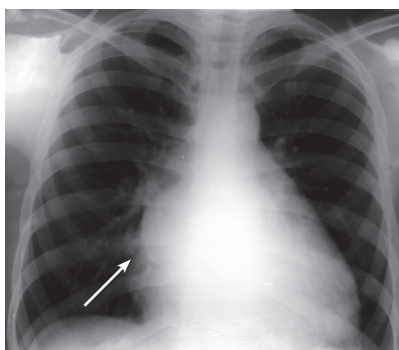
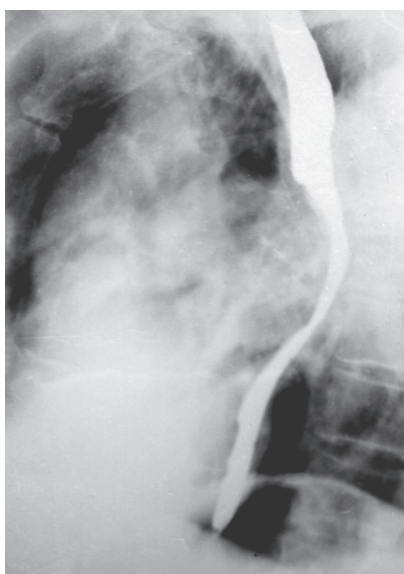
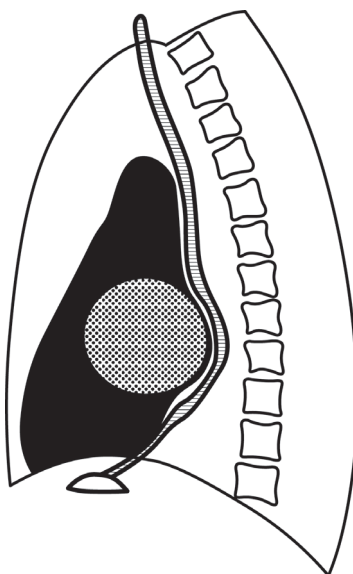


Fig. 9.20. Frontal X-ray. Enlargement of the left atrium (arrow)



a



b

Fig. 9.21. X-ray in the left lateral view with the enhanced esophagus (*a*) and scheme (*b*). Enlargement of the left atrium

parallel to the anterior surface of the spine. The enlargement of the left atrium causes a local deviation of the esophagus to the back: I degree of enlargement — the esophagus does not reach the spine, II degree — it reaches the spine, III degree — it is layered on the spine (Fig. 9.21).

Left ventricle. In the frontal view, the enlargement of the left ventricle causes arch elongation and nipple of the left border of the heart silhouette. In the left lateral view, the size of the left ventricle can be determined by the degree of the heart attachment



Fig. 9.22. X-ray in the left lateral view. The enlargement of the left ventricle

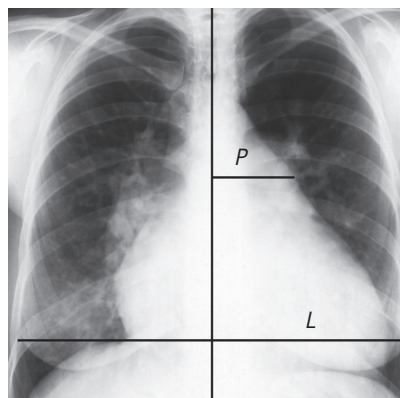


Fig. 9.23. Frontal X-ray with the designation of the measurement for determination of the degree of the pulmonary artery expansion: *L* — half of the transverse basal size of the chest; *P* — the distance from the median line to the most distant point of the pulmonary artery border

to the diaphragm. In normal condition, it does not exceed $1/4$ length of the diaphragmatic cupula. When it is elongated, subsequently, it increases, which leads to a narrowing of the lower part of the retrocardiac space. The main sign of the normal condition of the left ventricle in this projection is also acute posterior cardiophrenic angle and the image of the pulmonary ligament in it. With the enlargement of the left ventricle, the posterior cardiophrenic angle can become right or even obtuse, the isolated image of the pulmonary ligament disappears (Fig. 9.22).

The pulmonary artery is estimated in the frontal view by the distance between the medial line and the most distant point of its border. Regarding the half of the transverse basal size of the chest (*Moore's coefficient* $P/L \times 100\%$), this size in normal condition does not exceed 30%. With the expansion of the pulmonary artery of the I degree, this coefficient reaches 35%, II degree — 40%, III degree — more than 40% (Fig. 9.23).

Special roentgenopaque techniques

The angiocardiology is a technique of the artificial contrast study of the heart cavities. As a rule, The Seldinger technique is used to place central IV lines in femoral vein with the passing of the catheter in the inferior vena cava to reach the right chamber of the heart (Fig. 9.24). If exactly the left heart chambers should be enhanced, the left atrial is approached from the right one by means of interatrial septum puncture (Fig. 9.25). The main indication for angiography is the diagnosis of complex, combined heart defects if non-invasive methods are undecisive enough. They study the position, shape and size of the heart cavities; the sequence of their filling of the RCA, changes in the intensity and uniformity of their contrast, velocity of the RCA passing, the condition of the valve apparatus; the pathological connection between the heart

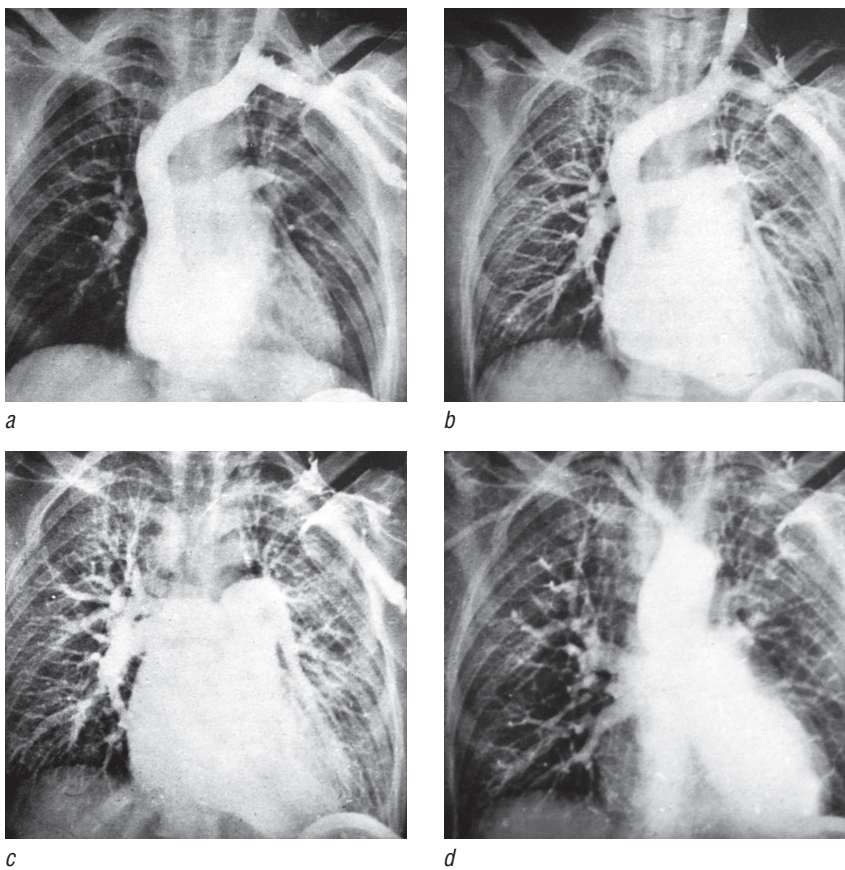


Fig. 9.24. Series of angiographic images with a consequential enhancement of the right cardiac chambers (a), vessels of the pulmonary circulation in the arterial phase (b), vessels of the pulmonary circulation in the venous phase (c), of the left chambers of the heart and thoracic aorta (d)

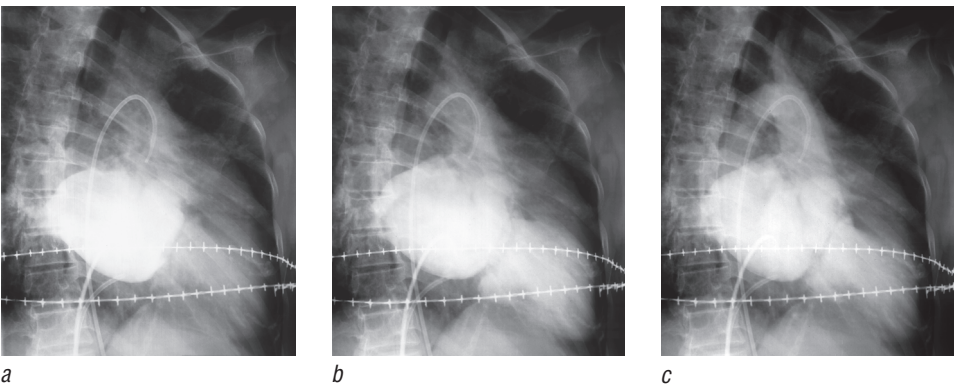
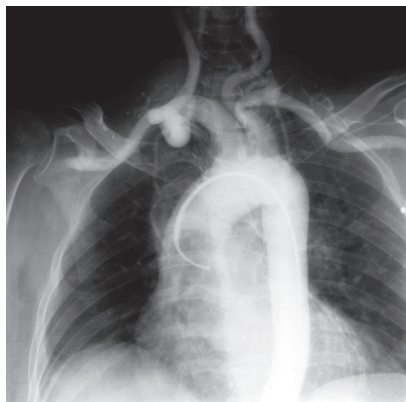
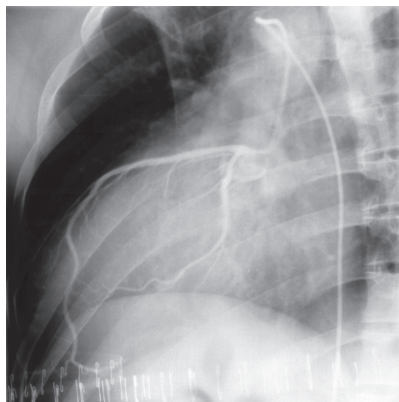


Fig. 9.25. Series of angiographic images with a consequential enhancement of the left atrium (a), left ventricle (b), aorta (c)

**Fig. 9.26.** Aortogram**Fig. 9.27.** Selective coronary angiogram

cavities is determined. At the same time, the intracardial pressure is measured; the gas composition of blood in various chambers of the heart, minute and shock volumes of the heart are determined; the intracardial ECG and PCG are recorded. All this allows giving a detailed not only qualitative but also quantitative description of the morphological changes of the heart and disorders of central hemodynamic.

Aortography — is an enhanced radiologic examination of the thoracic aorta, usually carried out by catheterization of the femoral artery with the catheter insertion in the initial part of the aorta (Fig. 9.26). It is highly informative in the diagnosis of aneurysms, occlusion, abnormalities of the thoracic aorta, differentiation of its lesions with tumors of the mediastinum. However, unlike ultrasound, CT and MRI it provides information only about the aortic lumen and does not allow determining the state of the vascular wall.

Coronography is an enhanced examination of coronary arteries in order to specify the character, localization of the vascular lesions and evaluation of collateral blood flow. It is used to decide the issue of the need, type and degree of surgical intervention in patients with coronary artery disease. The technique used for either general thoracic aortography with the catheter insertion in the initial part of the aorta, or, preferably, selective coronography with the successive catheterization of each coronary artery (Fig. 9.27). Currently, coronography is performed not only for diagnostic purposes but also as the first stage of interventional procedures — coronary intervention and stenting.

However, these invasive techniques are burdensome and even unsafe for the patient, so the indications for their use are significantly reduced now.

9.1.2. Ultrasound technique

Ultrasound is highly informative and is the main method of diagnosis of heart diseases nowadays. It allows estimating reasonably the morphological and functional state of all cardiac structures, their anatomical features, myocardial contractility, the state of central hemodynamics, that is, provides comprehensive and multifaceted information about the heart. The role of this method in assessing the state of the thoracic aorta is also quite important. The main indications for ultrasound are aortic

aneurysms, aortic coarctation, Marfan syndrome, occlusive lesions of the branches of the aortic arch.

In order to obtain the largest amount of information, complex ultrasound is needed. Thus, each case requires a different type of echocardiography: B mode, M-mode and Doppler ultrasonography.

The **B-mode** is a basic approach. This is an ultrasound scanning, which is carried out in real-time mode from different exposures and in different planes and slices. It allows obtaining images of all anatomical structures of the heart (ventricles, atria, valves) with follow-up assessment (of the chamber size, thickness and movement patterns of its walls and motion of cardiac valves) (Fig. 9.28–9.30). Thus, it is also possible to identify the pathological intracardiac masses. For the study of the thoracic aorta, the suprasternal access is used in order to obtain longitudinal and transverse images of the aortic arch, as well as branches deriving from it (Fig. 9.31).

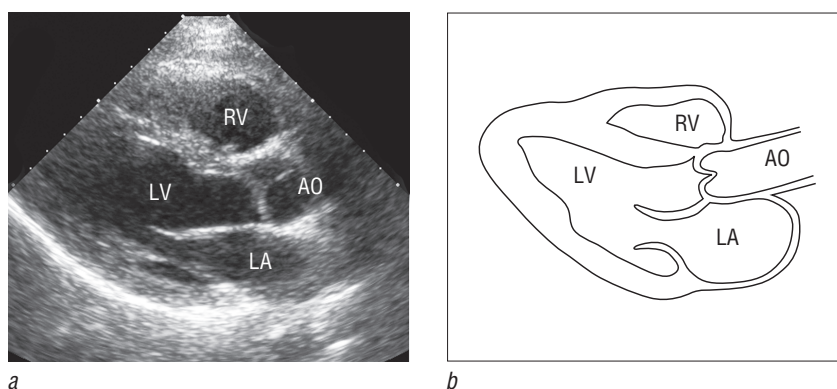


Fig. 9.28. Echocardiogram from the left parasternal long-axis view (a) and scheme (b). LV — left ventricle; RV — right ventricle; AO — aorta; LA — left atrium

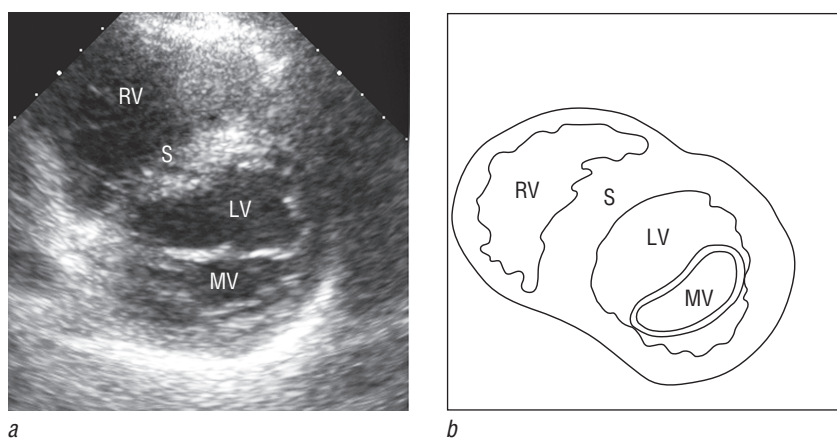


Fig. 9.29. Echocardiogram from the left parasternal short-axis view (a) and scheme (b). RV — right ventricle; S — ventricular septum; LV — left ventricle; MV — mitral valve

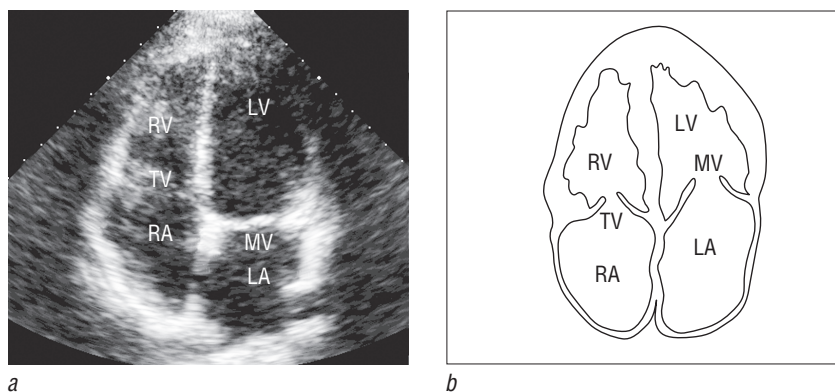


Fig. 9.30. Echocardiogram from the apical four-chamber view (a) and scheme (b). RV — right ventricle; LV — left ventricle; RA — right atrium; LA — left atrium; TV — tricuspid valve; MV — mitral valve

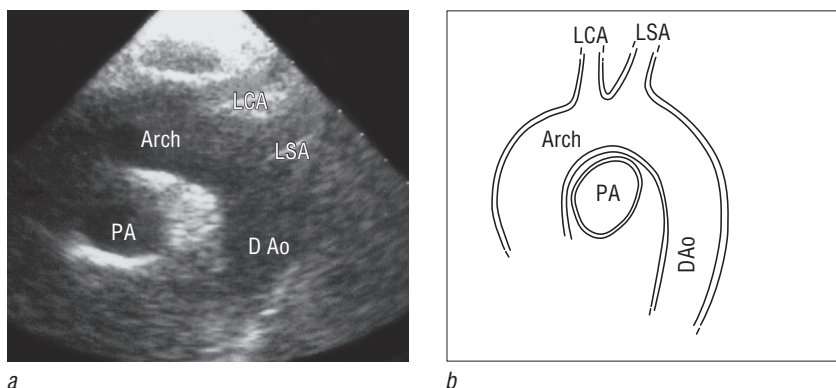


Fig. 9.31. Echocardiogram from the suprasternal long-axis view (a) and scheme (b). Arch — aorta arch; D Ao — descending aorta; LCA — left carotid artery; LSA — left subclavian artery; PA — a pulmonary artery

M-mode serves as an additional technique and allows measuring the heart biometrical data, first of all, the amplitude and speed of movement of cardiac structures.

Doppler echocardiography (DEchoCG). Nowadays flow, spectral, CDI and tissue Doppler ultrasonography are used in cardiological practice.

Spectral DEchoCG and CDI are used in examinations of the blood flows in heart cavities with a determination of their nature, direction and speed (Fig. 9.33). According to the spectrographic indicators of blood flow rates, it is possible to calculate such important indicators of central hemodynamics as stroke and minute output, cardiac index, pressure gradients.

An image received in CDI is a dimensional echocardiogram in randomly selected section with blood flows overlaid, which are encoded by different colors depending on their direction (Fig. 9.34, see colored insert). The main advantage of CDI is that it allows determining the spatial orientation and boundaries of both physiological and pathological blood flows accurately.

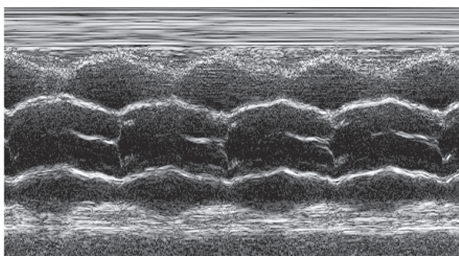


Fig. 9.32. Aortic valve cusps movement curve in M-mode

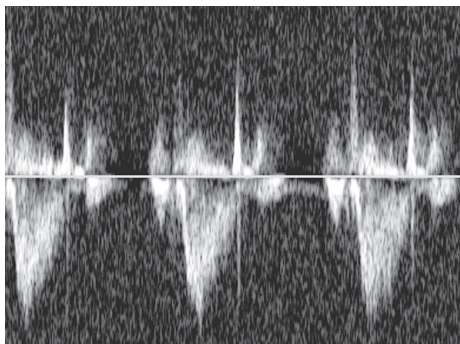


Fig. 9.33. Doppler spectrogram of transaortic bloodstream

Tissue Doppler ultrasonography in cardiology is mainly intended for the study of the physiological function of the myocardium. The echograms show the spatial distribution of the velocities of the certain elements of the heart muscle and the energy levels of the echoes from the moving tissues in color Doppler imaging (Fig. 9.35, see colored insert).

In general, the greatest clinical significance of the DEchoCG consists in revealing and assessment of the degree of valvar regurgitation, pathological shunts, in determination of the hemodynamic significance of stenosis, quantification of pulmonary arterial hypertension, determining the functional state of the heart chambers.

Transesophageal scanning and the use of stress tests (stress EchoCG) significantly expand the possibilities of echocardiography (EchoCG).

Transesophageal ultrasound of the heart is of great significance in atrial neoplasms, malformations in valve prostheses, infective endocarditis, congenital heart defects, thoracic aorta diseases. In addition, this study is highly effective in the assessment of the function of the left ventricle, in recognizing complications of myocardial infarction, in identifying intracardiac blood clots.

Stress echoCG is an ultrasound of the heart under additional load. The physical load (bicycle, treadmill), transesophageal electrical stimulation of the heart, pharmacological agents can serve as loading samples. The main purpose of stress-echoCG is to determine the reaction of the left ventricle to the load, to identify disorders that are not recorded at rest.

In clinical practice, ultrasound is also used to assess the state of the coronary arteries by intravascular catheterization using special microsensors. Only this technique provides information about the lumen of the vessel, and the state of its wall, and the nature and severity of the pathological changes in it, especially the length and depth of calcification, which is extremely important in the planning of balloon angioplasty.

9.1.3. X-ray computed tomography

CT of the heart and thoracic aorta can be performed under natural contrast conditions (native CT) or using artificial blood contrast (CT angiocardiography).

Native CT-study gives a general idea of the thoracic organs, including, of course, the heart and large vessels. In this case, the external outlines of the heart chambers are

visible, limited by fat layers. The cavities of the heart chambers are not differentiated in isolation since the density of blood in them is almost equal to the density of the myocardium. The ascending and descending parts of the thoracic aorta on the axial sections are displayed in the enumerative section; the aortic arch — in the longitudinal section.

In general, the native CT has low information capacity. The main indications for its targeted implementation are limited to the diagnosis of exudative and adhesive pericarditis and the detection of calcifications in the coronary arteries. The last issue is particularly relevant to:

- ▶ the selection of patients with coronary artery disease for coronary angiography;
- ▶ the determination of indications and contraindications for balloon angioplasty and prediction of its results;
- ▶ the assessment of the dynamics of atherosclerotic lesions of the coronary arteries in order to determine the effectiveness of the therapy.

The software of modern computed tomography scanners allows determining the area, volume, number of calcifications, as well as the mass of calcium phosphate. CT angiocardiology has much greater capabilities in assessing the state of the heart, coronary arteries and aorta. This technique is based on the artificial increase in the density of blood in the chambers of the heart and in the vessels, which provides a separate image of their cavities and walls. This study is performed by rapid IV bolus administration of 100–150 ml RCA at a speed of 3–4 ml/s. The study is carried out in the arterial phase. In order to catch it, the scan should be started in 15–20 seconds after the injection of the RCA. The image clarity of pulsating, rapidly shifting vessels and the heart is achieved by high scanning speed.

These requirements are met by multislice spiral computed tomography (MSCT) and cathode ray tomographs (CRT), which can synchronize with ECG. They allow visualising all structures of the heart with high spatial and temporal resolution (Fig. 9.36, 9.37). The study can be performed in the form of the static or dynamic scanning, that is, with the production at each level of single scans or series of tomograms. All series of images are subject to visual and densitometric analysis. The advantage of dynamic scanning is the ability to assess not only the morphological changes but also the state of central hemodynamics, mainly by the speed of passage of the RCA through the heart chambers. The additional, very important information is provided by multiplanar reformations and three-dimensional transformation.

In general, the MSCT and CRT examinations of the heart with enhancement ensure the reliable diagnosis of aneurysms, blood clots and intracavitary heart neoplasms, cicatricial myocardial affections, hypertrophic cardiomyopathy and other pathological conditions. In addition, this technique can be used for functional study of the heart: assessment of the volume of chambers, total and regional contractility, the rate of intracardiac blood flow, myocardial perfusion, as well as the detection of the pathological shunts and regurgitating flows.

In order to assess the condition of the coronary artery, the multiplanar reconstructions are used as well. The Max IP-projections can be carried out too, especially for proximal regions of the coronary arteries. However, volume-rendering technique (VRT) is the most informative one. In this study, in all cases, it is possible to obtain a clear image of the proximal and middle thirds of the coronary arteries and their large branches in 90% of all cases. Thus, the structural changes are revealed with high

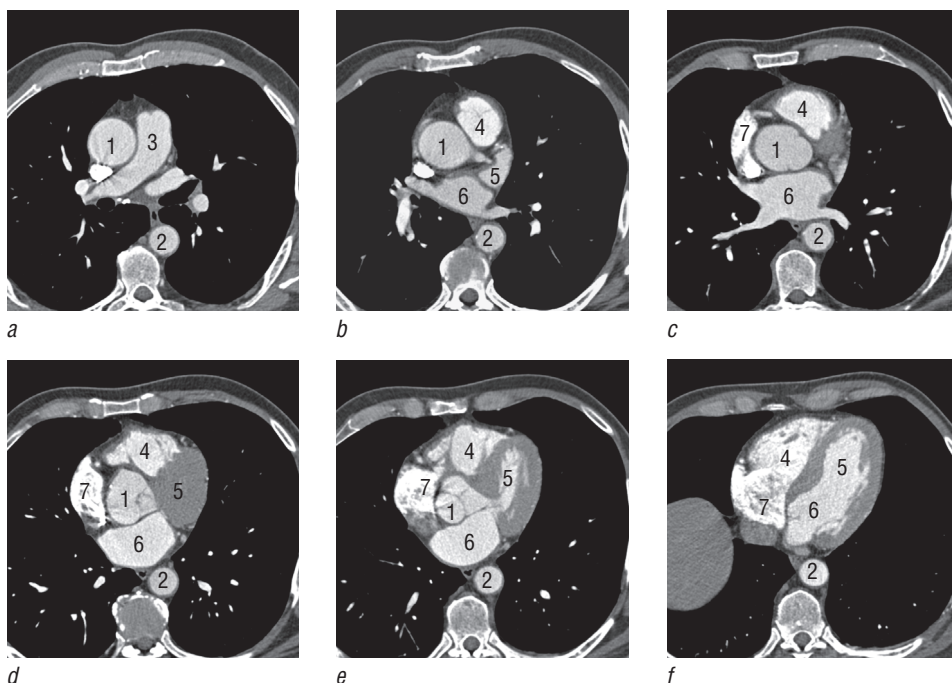


Fig. 9.36. Series of computer tomographic angiocardiograms at different levels of axial sections (*a–f*): 1 — ascending aorta; 2 — descending aorta; 3 — pulmonary artery; 4 — right ventricle; 5 — left ventricle; 6 — left atrium; 7 — right atrium

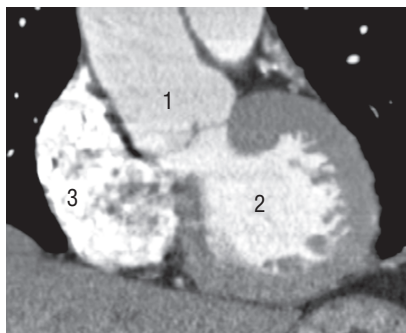


Fig. 9.37. Frontal computed tomographic angiogram: 1 — ascending aorta; 2 — left ventricle; 3 — right atrium

accuracy such as calcifications and stenoses of arteries (Fig. 9.38, see colored insert). However, the data from MSCT and CRT coronographies are still insufficient enough to meet operational and interventional vascular procedures. The main disadvantage of these technologies is poor visualization of the distal parts of the coronary arteries and their small branches. Metal stents in the coronary arteries make it impossible to assess the state of the vascular wall at their location.

Significantly fewer difficulties arise in assessing the state cardiac shunts, which are visualized along the entire length (Fig. 9.39, see colored insert). The dynamic CT can be used in the quantitative assessment of blood flow along the shunt. Virtual aortoscopy allows exploring the shunt ostia from the inner side of the aorta.

Enhanced MSCT and CRT provide an image of the whole thoracic aorta simultaneously (Fig. 9.40, see colored insert). These techniques provide the most sustainable information in the diagnosis of aneurysms, aortic dissection and developmental dis-

orders of the aorta (coarctation, congenital tortuosity and retroesophageal location of the arc, vascular ring, etc.). In terms of aneurysms of the thoracic aorta, this study considerably exceeds the capabilities of traditional radioopaque aortography, providing comprehensive information, which is necessary for surgical intervention, such as localization, diameter, length, the shape of the aneurysm and the correlations with the branches of the aorta; thrombotic masses, dissection, rupture of the wall; para-aortic hematoma.

9.1.4. Magnetic resonance imaging

Magnetic resonance imaging of the heart and coronary arteries is carried out simultaneously with the contractions of the heart and the phases of breathing in order to obtain a high-quality image. In the absence of such synchronization, only the outer outlines of the heart are visible. High spatial and temporal resolution is provided by the use of fast and ultrafast pulse sequences. They significantly expand the diagnostic capabilities of this technique. Some of them make it possible to obtain consistent images at the same level according to the different phases of the cardiac cycle, followed by a replay in a film mode, which makes it possible to study the contractility of the heart and the function of the valves. The modern model of MR-scanners allows obtaining multi-phase cine-MRI simultaneously in several anatomic levels. Ultra-fast sequences provide an opportunity to observe the passage of contrast medium through the heart chambers, as well as the distribution of the first bolus of contrast medium in the myocardium, which allows evaluating its perfusion in real-time.

MR heart examination usually starts with tomograms in the standard plane (Fig. 9.41).

Unlike CT, MRI provides a differentiated image of the walls of the heart and blood in its cavity, in native conditions. This is conditioned by the different level of MR-signals from these objects. Normal myocardium on MR-images gives an isointense signal (grey), pericardium — hypointense signal (black colour), adipose tissue yields the most intense signal and is white. The intensity of the myocardial MR-signal can

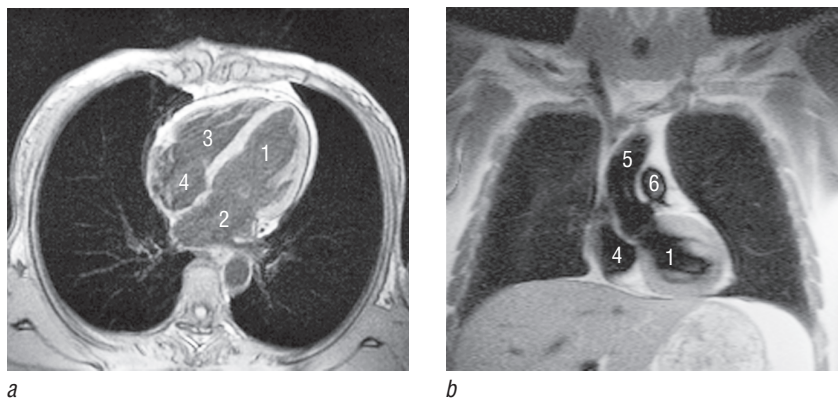


Fig. 9.41. Magnetic resonance images of the heart in axial (*a*) and frontal (*b*) planes: 1 — left ventricle; 2 — left atrium; 3 — right ventricle; 4 — right atrium; 5 — ascending aorta; 6 — pulmonary artery

serve as the basis for the estimation of its condition. The sufficiently clear image gets most of the main anatomical structures of the heart: myocardium, heart valves, papillary muscles, large trabeculae and pericardium. Coronary arteries in native MRI differ in fragments, so their evaluation with clinical objectives is not possible yet. The analysis of MR-images performed in different phases of cardiac activity allows evaluating ventricular function with the detection of such important indicators as systolic and end-diastolic volumes, ejection fraction; thickness, systolic thickening and mobility of the walls by segments. The data obtained correspond with the results of EchoCG, CT and angiocardiology well.

The enhancement technique in cardiology is mainly used in order to assess the perfusion and viability of myocardia. The quantitative characteristics of the accumulation and excretion of contrast agents are determined by the generation of the intensity-time curve, which indicates the changes in MR-signal level in the area under study throughout the whole period of examination. The perfusion defects are manifested by the signal weakening and delayed administration of contrast agents into the affected area of the myocardium. This data is used in the diagnosis of the acute infarction and cicatricial myocardial damage, apical hypertrophic cardiomyopathy and myocarditis.

Contrast MR coronary angiography is inferior to multilayer spiral CT and electron beam tomography in terms of informational content. Nevertheless, it can be carried out for the diagnosis of stenoses, occlusions and abnormalities of coronary arteries. The quality of the images is improved in three-dimensional reconstruction.

MR examination of the thoracic aorta is carried out without synchronizing with the heart contractions. In order to obtain a complete image of the aorta, the plane that is parallel to the aortal arch is chosen.

In general, MRI should be considered as a technique of cardio imaging study with a high informational capacity. It remains a priority in the diagnosis of heart and aortic aneurysms, aortic coarctation, paracardial neoplasms and hypertrophic cardiomyopathy. MRI makes it possible to detect with high accuracy cicatrice myocardial damage, heart and aortic blood clots, pathological intracardial shunts, stenosis and aortic valve insufficiency, aortic wall dissection. In addition, MRI helps to visualize the zone of myocardial infarction in the acute period and reliably differentiate exudate and transudate with blood accumulations in the pericardial cavity. However, it must be admitted that other radiation techniques, more economical and affordable have the same opportunities in the detection of some diseases and in the assessment of the functional state of the heart. In this regard, the indications for the use of MRI in each case should be fully justified.

9.1.5. Radionuclide method

The radionuclide method plays a significant role in the complex radiological study of the heart. It gives a comprehensive description of the morphological and functional changes of the heart. In order to solve certain diagnostic problems, some or other special techniques are used. The basic techniques are:

- ▶ myocardial perfusion scintigraphy;
- ▶ focal myocardial infarction scintigraphy;
- ▶ equilibrium radionuclide ventriculography.

Myocardial perfusion scintigraphy is based on the RP, which are selectively accumulated in intact tissue of the cardiac muscle proportionally to the intensity of the coronary flow. Thus, it is possible to study the blood supply to the heart at the level of microcirculation. In normal condition, a uniform intensive accumulation of the drug in the myocardium of the left ventricle is determined (Fig. 9.42, see colored insert). In the areas of the myocardium with reduced blood flow, the accumulation of RP is reduced, and in necrotic, cicatrice areas it is completely absent (negative scintigraphy).

Diffusive myocardial perfusion disorders are characterised by uneven inclusion of RP] over the entire area of the image. Important diagnostic information is provided by additional research in conditions of physical or pharmacological load. This makes it possible not only to determine the presence, location and extent of perfusion defects but also to assess the functional reserves of myocardial blood supply and to differentiate the zones of ischemic and infarction damage to the heart muscle.

Technically, myocardial scintigraphy is usually performed in the version of the SPECT. PET has even greater capabilities in the study of cardiac muscle perfusion and, in addition, provides information about myocardial metabolism.

Focal myocardial infarction scintigraphy, unlike myocardial perfusion scintigraphy, is based on the use of RP that, on the contrary, have tropism to the damaged and not to the intact myocardium (positive scintigraphy). The widest clinical application was gained by ^{99m}Tc -pyrophosphate. Reliable local inclusion of this radionuclide in the lesion occurs not earlier than 10 hours after the appearance of the first clinical signs of the heart attack and remains at a sufficient level within 5–6 hours. In these terms, the sensitivity of scintigraphy with ^{99m}Tc -pyrophosphate in the diagnosis of the acute myocardial infarction reaches 98%. Thus, in cases of suspected myocardial infarction in the first hours of its development, perfusion scintigraphy is indicated, and in 12–24 hours, it is more advisable to conduct research with RP, with tropism to the necrotized tissue.

Equilibrium radionuclide ventriculography is carried out with the use of the technique of red blood cells labelled in vivo. At first, the stanum pyrophosphate is administered to the patient; it actively absorbs on the red blood cells. In 20–30 minutes, the sodium pertechnetate [^{99m}Tc] is introduced, which aggregates with pyrophosphate at once. As a result, a stable label of at least 90% of the red blood cells for a period of up to 4 hours is provided.

After the complete dilution of RP in blood, single crystal scintillation camera captures several hundreds of images on the basis of which a single average pattern of the cardiac cycle is formed by computer analysis. Apart from the scintigraphic pattern, activity-time curves are constructed over the selected areas of interest in the projection of the left ventricle, which integrally reflects the contractile function of the heart for several cardiac cycles.

According to the difference in the levels of blood radioactivity in the ventricular cavities in the end-diastolic and end-systolic phases, their ejection fraction is calculated. The visualization of images of the heart in different phases makes it possible to assess the movement of the ventricular walls and as a result to identify regional violations of myocardial contractility.

The main indications for equilibrium radionuclide ventriculography are coronary heart disease, myocardial infarction, heart aneurysms, hypertense disease and diffuse

Table 9.1. Informative methods of radiation diagnosis in the detection of heart and thoracic aorta lesions

Signs	Techniques of diagnostic radiology					Priority technique
	EchoCG	CT	MRI	Roentgenopaque techniques	Radionuclide technique	
Heart						
Morphological changes	+++	+++	+++	++	+	EchoCG
Functional status	+++	++	++	++	++	EchoCG
Valve function	+++	+	+	+	—	EchoCG
Coronary arteries	—	++	+	+++	—	Roentgenopaque coronography
Perfusion and myocardial metabolism	—	+	+	—	+++	Radionuclide technique
Thoracic aorta	++	+++	+++	++	+	MRI, CT

Note: “+” — degree of informativeness (“+” — the lowest degree, “+++” — the highest degree); “–” — not informative.

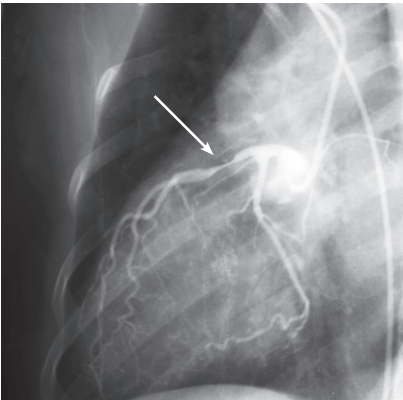
lesions of the heart muscle. The use of graduated exercise allows assessing the reserve capacity of the myocardium by ejection fraction.

The diagnostic significance of different radiological methods in cardiology is shown in table 9.1.

Thus, in diagnostic radiology of the heart, the most preferable and basic technique is EchoCG. In order to assess the perfusion and myocardial metabolism, the radionuclide examination is used. The “gold standard” of the assessment of coronary artery condition is the traditional roentgenopaque examination. The priority techniques in the diagnosis of thoracic aorta diseases are MRI and CT.

9.2. RADIOLOGICAL SEMIOTICS OF THE HEART AND THORACIC AORTA DISEASES

9.2.1. Coronary heart disease



EchoCG: the contractility disorder of certain regions of the left ventricle wall in the form of the reduced amplitude of movement and degree of systolic myocardial thickening; reduction of the ejection fraction of the left ventricle.

Myocardial perfusion scintigraphy: myocardial areas with reduced accumulation of RP (Fig. 9.43, see colored insert).

Fig. 9.44. Selective coronary angiogram. Stenosis of the anterior interventricular branch of the left coronary artery

Contrast X-ray and CT coronary angiography: narrowing, occlusion of various branches of the coronary arteries (Fig. 9.44).

9.2.2. Acute myocardial infarction

Myocardial perfusion scintigraphy: the complete absence of RP accumulation in the necrotized area of the myocardium (negative scintigraphy) (Fig. 9.45, see colored insert).

Focal myocardial infarction scintigraphy: area of RP hyper fixation (positive scintigraphy).

Equilibrium radionuclide ventriculography, EchoCG: akinetic area of the left ventricle wall; reduction of the ejection fraction of the left ventricular.

9.2.3. Mitral stenosis

Radiography: frontal view — nipple of the second and third arches of the left contour along the heart silhouette; there is an additional arch along the right contour of the heart silhouette in the area of the cardiovascular angle (contour of the hypertrophic enlarged left atrium); the upward displacement of the right cardiovascular angle; pulmonary changes as a result of pulmonary artery hypertension — an extension of the roots of the lungs due to the main and lobar branches of the pulmonary artery and vice versa, depletion of lung markings on the periphery as a result of spasm of small pulmonary arteries (a symptom of calibre leap) (Fig. 9.46).

The left lateral view shows the local displacement of the esophagus backwards by the enlarged left atrium; increase of the fit of the right ventricle to the sternum.

EchoCG: B-mode — domed diastolic deflection of mitral valve leaflets into the cavity of the left ventricle; reduction of mitral orifice area; thickening, induration, calcification of mitral valve leaflets (Fig. 9.47).

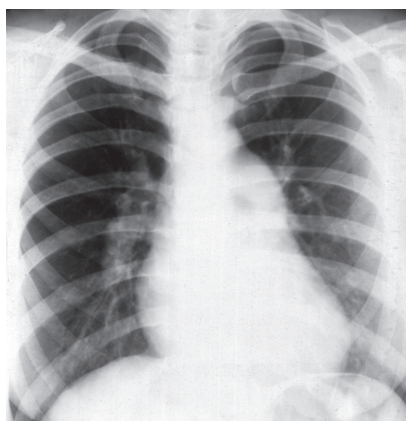


Fig. 9.46. Frontal X-ray. Mitral stenosis

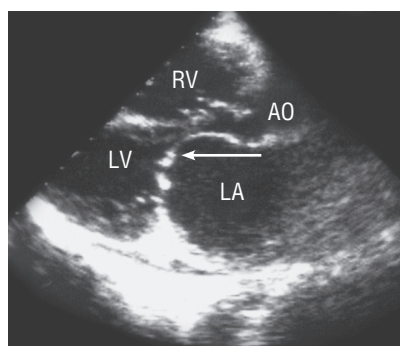


Fig. 9.47. Echocardiogram in B-mode. Mitral stenosis (arrow). LV — left ventricle; RV — right ventricle; AO — aorta; LA — left atrium

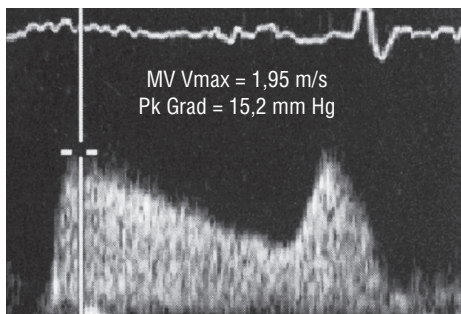


Fig. 9.48. Echocardiogram in M-mode.
Mitral stenosis

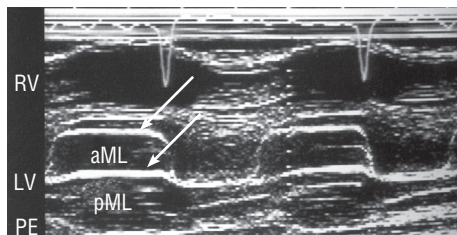


Fig. 9.49. Doppler spectrogram. Mitral stenosis (arrow). RV — right ventricle; LV — left ventricle; PE — pericardial effusion; aML — anterior mitral valve leaflet; pML — posterior mitral valve leaflet

M-mode shows the decrease in speed of early diastolic closing of the anterior mitral valve leaflet; the unidirectional diastolic movement of the mitral valve leaflets (Fig. 9.48).

Doppler echoCG shows the increase in the maximum speed of the mitral flow; increase in the diastolic gradient of the pressure between left atrium and ventricle (Fig. 9.49).

9.2.4. Mitral valve insufficiency

Radiography: frontal view — enlargement and displacement of the left ventricle arch to the left; nipple of the left atrial appendage in the left contour; displacement of the right border of the heart silhouette to the right due to the emergence of the enlarged left atrium; displacement of the right cardiovascular angle upwards.

The left lateral view shows the enlargement of the heart silhouette towards the spine and its wide adhesion to the diaphragm; enlargement of the posterior phreno-pericardial angle (Fig. 9.50).

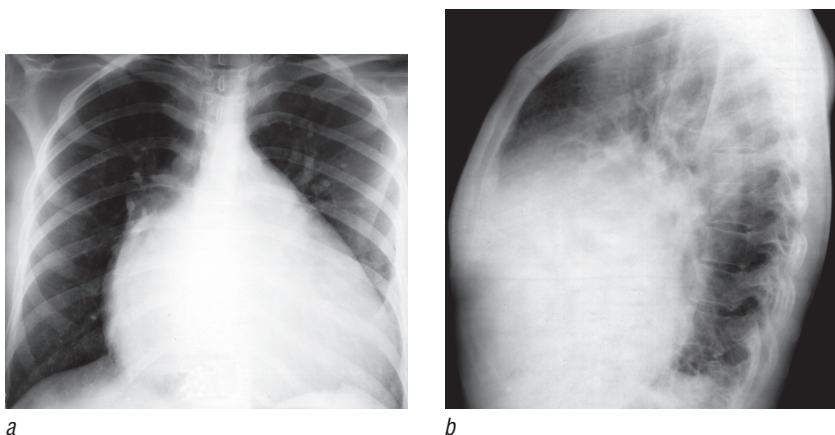


Fig. 9.50. X-rays in frontal (a) and left lateral (b) views. Mitral valve insufficiency

EchoCG: B-mode shows incomplete systolic closure of mitral valve leaflets; dilatation of the left heart chambers cavities.

Doppler echoCG: regurgitant blood flow throws the mitral valve from the left ventricle to the left atrium (Fig. 9.51, see colored insert).

9.2.5. Aortic valve stenosis

Radiography: in frontal view, there is an elongation and left shift of the left arch of the ventricle, extension of the arch of the ascending aorta; down-shift of the right cardiovascular angle.

The left lateral view shows the displacement of the left ventricle arch to the spine; extension of the ascending aorta, which leads to the narrowing of the retrosternal area at this level (Fig. 9.52).

EchoCG: B-mode shows the reduction of systolic divergence of aortic valve leaflets; thickening, induration, calcification of the aortic valve; reduction of the area of the aortic ostium.

Doppler echoCG: increased maximum aortic blood flow rate; increased systolic pressure gradient on the aortic valve.



Fig. 9.52. Frontal X-ray. Sclerosis of the aortic ostium

9.2.6. Aortic valve insufficiency

Radiography: frontal view shows enlargement and shift of the left ventricle arch to the left; extension of the arch of ascending aorta; down-shift of the right cardiovascular angle.

The left lateral view shows a shift of the left ventricle arch towards the spine; extension of the ascending aorta, which leads to the narrowing of retrosternal cavity at this level.

X-ray contrast aortography is a visualization of the regurgitant blood flow from the aorta to the left ventricle (Fig. 9.53).

EchoCG: B-mode shows incomplete diastolic closure of the aortic valve leaflets; dilatation of the left ventricle cavity; M-mode shows diastolic high-frequency small-amplitude fibrillation of the anterior aortic valve leaflet.

Doppler echoCG shows regurgitant blood flow throw the aortic valve from the aorta to the left ventricle (Fig. 9.54, see colored insert).

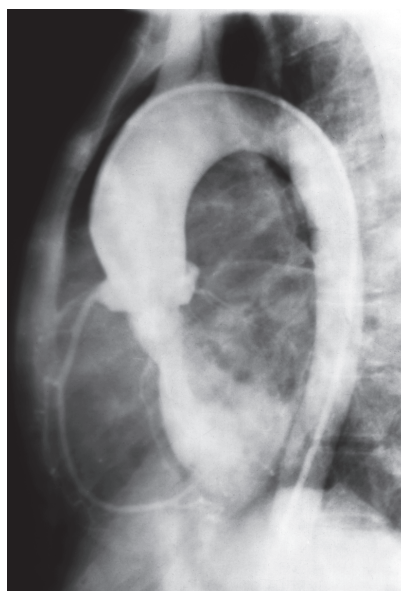


Fig. 9.53. Aortogram. Aortic valve insufficiency

9.2.7. Pericardial effusion

Radiography: the general enlargement of the heart silhouette, which takes a round shape; the disappearance of the arch along the borders of the heart silhouette; shortening of the vascular bundle; expansion of the superior vena cava (Fig. 9.55).

EchoCG, CT and MRI show the direct visualization of the liquid in the pericardial cavity (Fig. 9.56, 9.57).

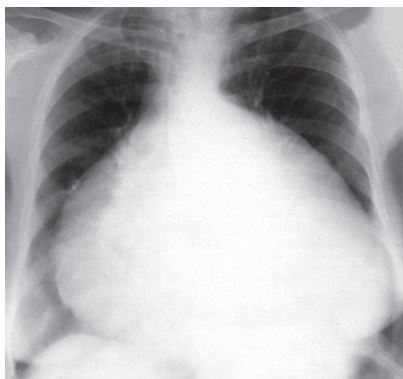


Fig. 9.55. Frontal X-ray. Pericardial effusion

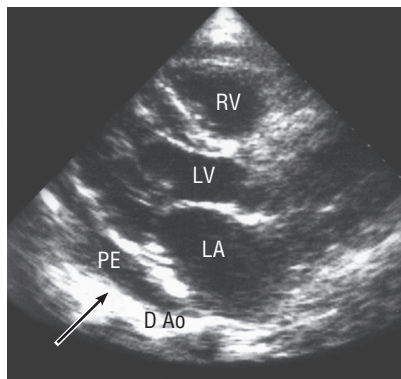
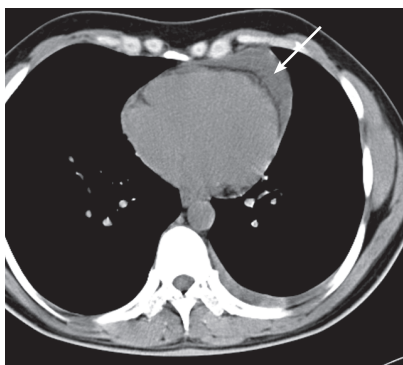


Fig. 9.56. Echocardiogram. Pericardial effusion (arrow). RV — right ventricle; LV — left ventricle; PE — pericardial effusion; LA — left atrium; D Ao — descending aorta



a



b

Fig. 9.57. Native computed tomographic image (*a*) and CT angiogram (*b*). Pericardial effusion (arrows)

9.2.8. Adhesive constrictive pericarditis

Radiography and fluoroscopy: calcification of pericardium; changes in shape and decrease in size of the heart silhouette; expansion of the superior vena cava; lack of pulsation along the heart silhouette with preservation of pulsation along the aorta borders (Fig. 9.58).

CT: thickening, induration, calcification of the pericardium.

EchoCG: lack of pericardial movements; the paradoxical movement of the ventricular septum towards the early diastole; the collapse of the inferior vena cava after the full inspiration less than 50%.

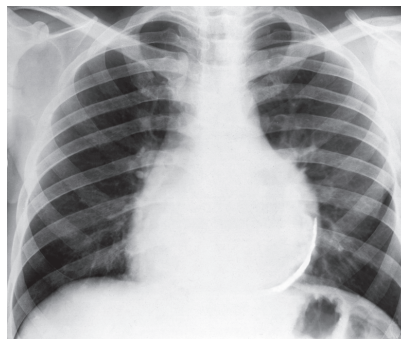


Fig. 9.58. Frontal X-ray. Adhesive constrictive pericarditis with calcification

9.2.9. Thoracic aorta aneurysms

Frontal X-ray shows a local expansion of the upper part of the medial shadow of semi-round, semi-oval shape with even and distinct borders, which cannot be separated from the aorta in any plane and has its own pulsation (Fig. 9.59).

MR aortography, contrast CT aortography allows not only to reveal aneurysm with high precision but also to define it comprehensively (shape, diameter, length, condition of para-aortic tissues, thrombotic masses, dissection) (Fig. 9.60).

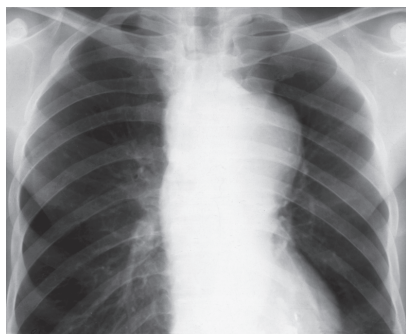


Fig. 9.59. Frontal X-ray. Aneurysm of the descending part of the aorta

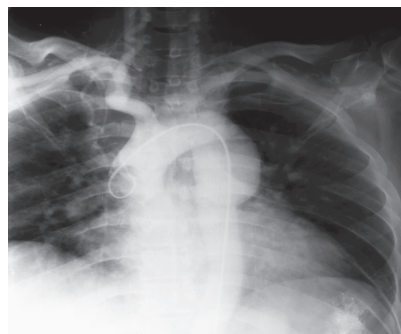


Fig. 9.60. Aortogram. Aneurysm of the descending part of the aorta

X-ray contrast aortography is limited by the ability to estimate only the aortic lumen. Moreover, as it is an invasive method of examination, there is a high risk of quite severe complications (embolism of cerebral arteries, rupture of the aneurysm sac).

9.3. RADIOLOGICAL SEMIOTICS OF THE HEART AND THORACIC AORTA INJURES

9.3.1. Contusion of the heart

EchoCG: regional worsening in contractility and decrease in ejection fraction of the ventricles; the area of contusion of the myocardium is of inhomogeneous echo-structure with inclusions of small echo-free areas due to the swelling and hemorrhage.

Myocardial perfusion scintigraphy: myocardial areas with a decrease in RP accumulation.

9.3.2. Rupture of the external walls of the heart

EchoCG, CT, MRI: direct visualization of fluid (blood) in the pericardial cavity.

Radiography: the overall increase of the heart silhouette acquires a spherical shape; smoothed arches on the contours of the heart silhouette; shortening of the vascular bundle; extension of the superior vena cava.

9.3.3. Rupture of the thoracic aorta

MR aortography, contrast-enhanced CT aortography: discontinuity, aortic wall dissection; pseudoaneurysm formation; the exit of contrast agent outside the aorta.

Practice questions

1. What is the position of the heart silhouette on the X-ray, depending on the constitutional type, breathing phase and body position of the examined patient?
2. What are the options for the pathological form of cardiovascular shadow on frontal X-ray?
3. Name the radiopaque techniques for the study of the heart and major vessels.
4. What is the most common technique of radiation diagnosis used in heart diseases?
5. What techniques are used in the echographic examination of the heart?
6. What is the technique of contrast enhancement in MRI?
7. What technique of radiation diagnosis is used to assess myocardial perfusion and metabolism?